Application of the discontinuous Galerkin method to 3D compressible RANS simulations of a high lift cascade flow

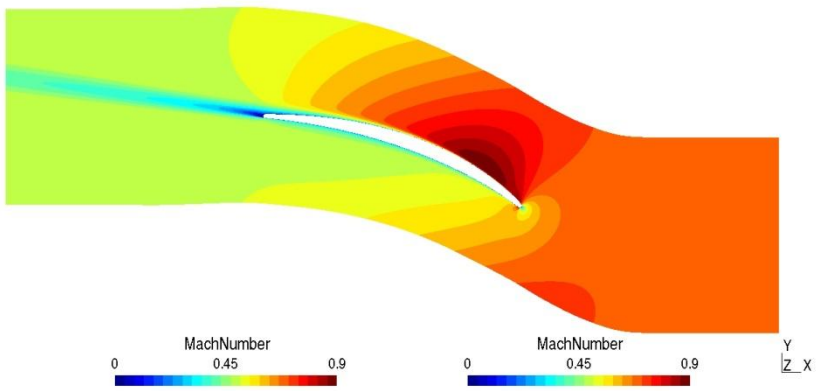

M. Drosson (ULg)

B. Gorissen (Cenaero)

K. Hillewaert (Cenaero)

March 25th 2011

Outline

- Discontinuous Galerkin method
- Spalart-Allmaras turbulence model
- Stability issues
- Grid convergence: flat plate
- 3D high lift cascade flow

Discontinuous Galerkin method

- Convection-diffusion-source equation

$$\frac{\partial u_m}{\partial t} + \mathcal{L}_m(u) = \mathcal{S}_m(u, \nabla u), \qquad m = 1 \dots N_v$$

with

$$\mathcal{L}_m(u) = \nabla \cdot \vec{f}_m(u) + \nabla \cdot \vec{d}_m(u, \nabla u)$$

- Variational principle

state function ϕ_i
state variable $\tilde{u}_m$

$$\mathbf{r}_{im} = (\phi_i, (\mathcal{L}_m(\tilde{u}) - \mathcal{S}_m(\tilde{u}, \nabla \tilde{u}))$$

$$= \int_\Omega \phi_i \cdot \left(\nabla \cdot \vec{f}_m(\tilde{u}) + \nabla \cdot \vec{d}_m(\tilde{u}, \nabla \tilde{u}) - \vec{S}_m(\tilde{u}, \nabla \tilde{u}) \right) dV$$

Discontinuous Galerkin method

- Notations
  - Jump [ ] and average <> operator

$$[u] = u^+ \vec{n}^+ + u^- \vec{n}^-$$
$$\langle u \rangle = (u^+ + u^-)/2$$

  - Riemann solver

$$\mathcal{H}(\tilde{u}^-, \tilde{u}^+, \vec{n})$$

  - Diffusive flux

$$d_m^k = \sum_{l=1}^{d} D_{mn}^{kl} \frac{\partial u_n}{\partial x_l}$$

Discontinuous Galerkin method

- Interior penalty method

$$\mathbf{r}_{im} = \underbrace{-\int_{\mathcal{T}} \nabla\phi_i \cdot \vec{f}_m \, dV}_{CV} \underbrace{-\int_{\mathcal{T}} \nabla\phi_i \cdot \vec{d}_m \, dV}_{DV} \underbrace{-\int_{\mathcal{T}} \phi_i \cdot \vec{S}_m \, dV}_{SV}$$
$$+ \underbrace{\oint_{\partial\mathcal{T}} \phi_i \mathcal{H}_m(\tilde{u}^-, \tilde{u}^+, \vec{n}) \, dS}_{CI} + CBD$$
$$+ \underbrace{\oint_{\partial\mathcal{T}} [\phi_i]^k \left\langle D^{kl}_{mn} \cdot \frac{\partial \tilde{u}_n}{\partial x_l} \right\rangle dS}_{DI} + \theta \underbrace{\oint_{\partial\mathcal{T}} [\tilde{u}_n]^k \left\langle D^{kl}_{nm} \cdot \frac{\partial \phi_i}{\partial x_l} \right\rangle dS}_{DT}$$
$$+ DBD + DBN$$
$$+ \underbrace{\oint_{\partial\mathcal{T}} \sigma[\tilde{u}_m][\phi_i] \, dS}_{DP} + PBD$$

θ = +1 → SIPDG
θ = -1 → NIPDG

Spalart-Allmaras model

- Spalart-Allmaras turbulence model
  - **One equation model** based on empiricism and arguments of dimensional analysis
  - Developed and calibrated for flows like airfoils and wings
  - Working variable $\tilde{\mu}$ (linear behaviour near the wall)

$$\mu^t = \tilde{\mu} f_{v1}, \qquad f_{v1} = \frac{\chi^3}{\chi^3 + c_{v1}^3}, \qquad \chi = \frac{\tilde{\mu}}{\mu}$$

$$\frac{\partial \tilde{\mu}}{\partial t} + \frac{\partial (\tilde{\mu} u_j)}{\partial x_j} - \frac{1}{\sigma} \frac{\partial}{\partial x_j} \left[(\mu + \tilde{\mu}) \frac{\partial (\frac{\tilde{\mu}}{\rho})}{\partial x_j} \right] = Q^{SA}$$

Spalart-Allmaras model

- Source term

$$Q^{SA} = \underbrace{c_{b1}\tilde{\omega}\tilde{\mu}}_{production} \underbrace{- \rho\left(c_{w1}f_w - \frac{c_{b1}}{c_\kappa^2}f_{t2}\right)\left(\frac{\tilde{\mu}}{\rho d}\right)^2}_{destruction} + \underbrace{\frac{1}{\sigma}\left[\rho c_{b2}\frac{\partial\left(\frac{\tilde{\mu}}{\rho}\right)}{\partial x_j}\frac{\partial\left(\frac{\tilde{\mu}}{\rho}\right)}{\partial x_j}\right]}_{diffusion}$$

$$c_{v1} = 7.1,\ c_{v2} = 5.0,\ c_{b1} = 0.1355,\ c_{b2} = 0.622,$$
$$c_{w1} = 3.2391,\ c_{w2} = 0.3,\ c_{w3} = 2.0,\ c_\kappa = 0.41,\ \sigma = 2/3$$

Spalart-Allmaras model

- Production term: $\rho c_{b1}(1-f_{t2})\tilde{\omega}\tilde{\nu}^*$

Modified vorticity : $\tilde{\omega} = |\omega| f_{v3} + \frac{\tilde{\nu}^*}{c_\kappa^2 d^2} f_{v2}$

$$f_{v2} = \left(1 + \frac{\chi}{c_{v2}}\right)^{-3} \qquad f_{v3} = \frac{(1+\chi f_{v1})(1-f_{v2})}{\chi}$$

- Destruction term: $-\rho\left(c_{w1} f_w - \frac{c_{b1}}{c_\kappa^2} f_{t2}\right)\left(\frac{\tilde{\nu}^*}{d}\right)^2$

$$f_w = g\left(\frac{1+c_{w3}^6}{g^6 + c_{w3}^6}\right)^{1/6} \qquad g = r + c_{w2}(r^6 - r) \qquad r = \frac{\tilde{\nu}^*}{\tilde{\omega} c_\kappa^2 d^2}$$

Stability issues

- Given the previous definitions, it is easy to see that the Spalart-Allmaras model becomes **unstable** for negative turbulent viscosities.

$$\lim_{\chi \to -c_{v1}} f_{v1} = \infty$$

$$\lim_{\chi \to -c_{v2}} f_{v2} = \infty$$

Latter are frequently observed in the outer boundary layer, if the grid resolution is insufficient.

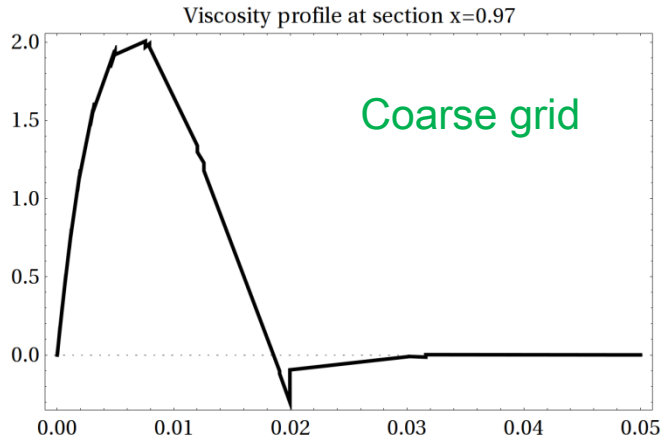

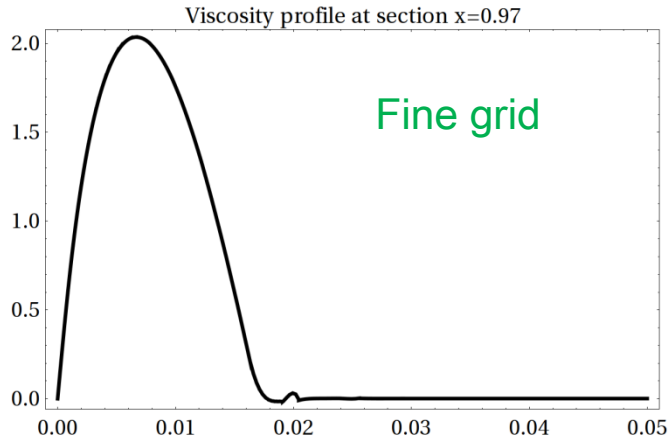

Stability issues

- Possible solutions :
  - Increase the grid resolution
    1. Grid refinement
    2. Use of high order methods

1. <u>Modification of the turbulence model,…</u>
   1. Approximate Jacobian (Spalart & Allmaras ‘91)
   2. Artificial viscosity (Ngyen, Person & Perraire ‘07)
   3. Clipping (Landmann et al ‘07)
   4. Modification of the turbulence model in order to ensure a decrease in time of the negative turbulent energy (Oliver ‘08)

→ HERE: LOCAL CLIPPING

Stability issues – Interior penalty

2. Modification of the transpose term

- Original version: breakdown due to negative densities after some iterations
- Likely reason: fast growing of the turbulent variable near the leading edge affects the continuity equation
- Remedy: decouple the SA model and the continuity equation

$$DT_{modif} = \theta \oint_{\Gamma} \begin{pmatrix} \left\langle n_k \, D^{kl}_{11} \, \frac{\partial \phi_i}{\partial x_l} \right\rangle & \cdots & \mathbf{0} & \mathbf{0} \\ \vdots & \ddots & \vdots & \vdots \\ \left\langle n_k \, D^{kl}_{1N_v} \, \frac{\partial \phi_i}{\partial x_l} \right\rangle & \cdots & \cdots & \left\langle n_k \, D^{kl}_{N_v N_v} \, \frac{\partial \phi_i}{\partial x_l} \right\rangle \end{pmatrix} \begin{bmatrix} [\rho] \\ \vdots \\ [\tilde{\mu}] \end{bmatrix} dS$$

Stability issues – Interior penalty

3. Different choices for the penalty coefficient

– Penalty coefficient : $\sigma = C_{IP}\frac{\nu}{h}$

ν : viscosity

h : element size

– C_{IP} : “constant” depending on the interpolation order p and the dimension d (→ Shahbazi ‘05)

$$C_{IP} = \frac{(p+1)\cdot(p+d)}{d}$$

– Different choices for h (→ K. Hillewaert FEF 2011)

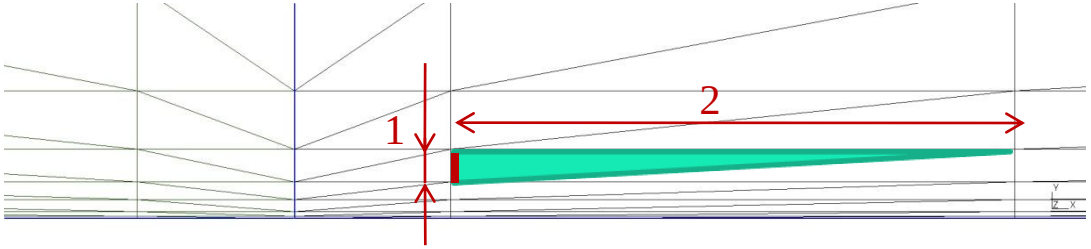

1 : quotient volume/surface (Shahbazi)

2 : distance to oppposing node

Test case: Flat plate

- Flat plate

  Re = 5 ×10^6
  M = 0,2
  L_x = 2

- Grid convergence
  - 2 types of grids

    (structured triangles/quadrangles)
  - Number of elements

    y+=4: (5+16) × 15

    … …

    y+=128: (5+16) × 8
  - Velocity profile / Friction coefficient / convergence order

$$u^+ = U/u_\tau$$
$$y^+ = u_\tau y/\nu$$
$$u_\tau = \sqrt{\tau_w/\rho}$$

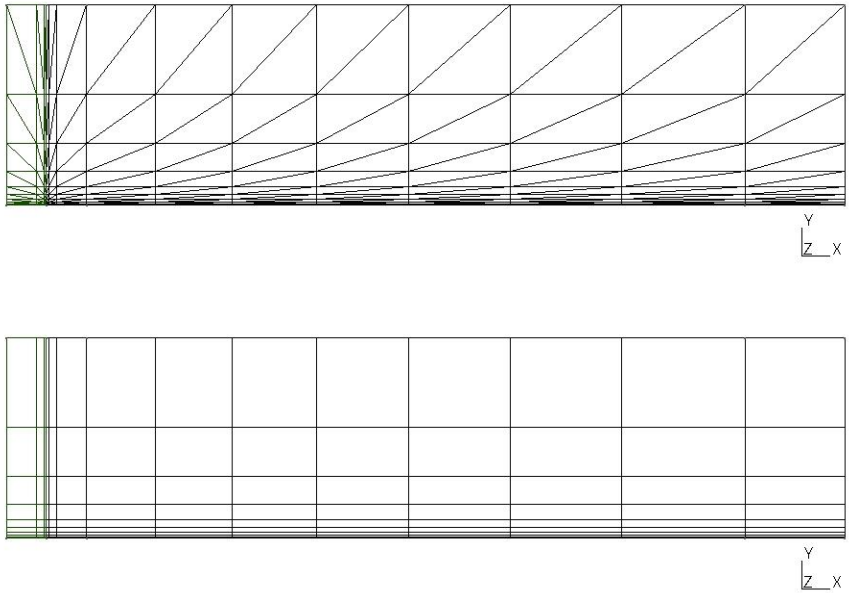

Grid stretching: 1.6

For the visualization, the grids have been scaled by a factor 10 in y direction.

Computed friction (structured quads)

- Physical (consistent) vs numerical skin friction
  - Important improvement of the skin friction Cf by taking into account the penalty term

Physical

$$\vec{d}_m = \left\langle D^{kl}_{mn} \cdot \frac{\partial \tilde{u}_n}{\partial x_l} \right\rangle$$

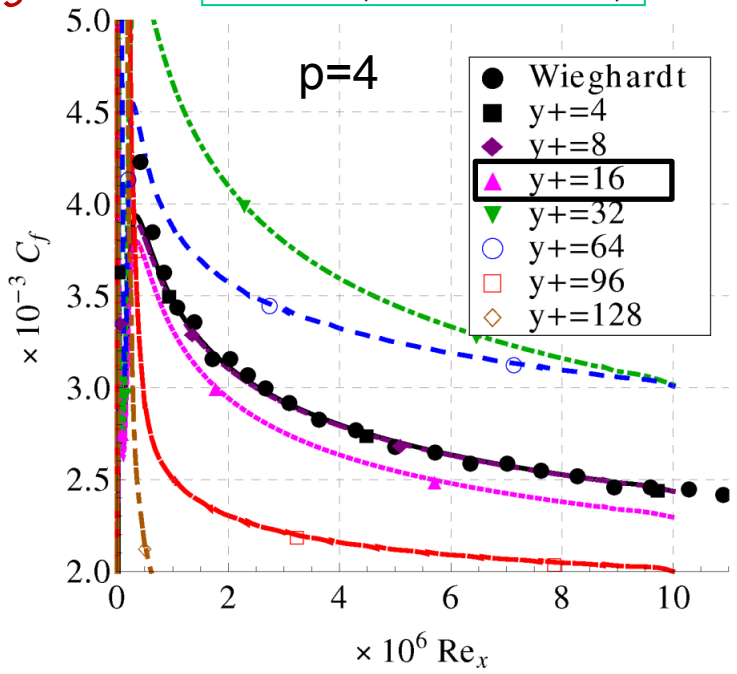

Numerical

$$\hat{d}_m = \left\langle D^{kl}_{mn} \cdot \frac{\partial \tilde{u}_n}{\partial x_l} \right\rangle + \sigma\,[\tilde{u}_m]$$

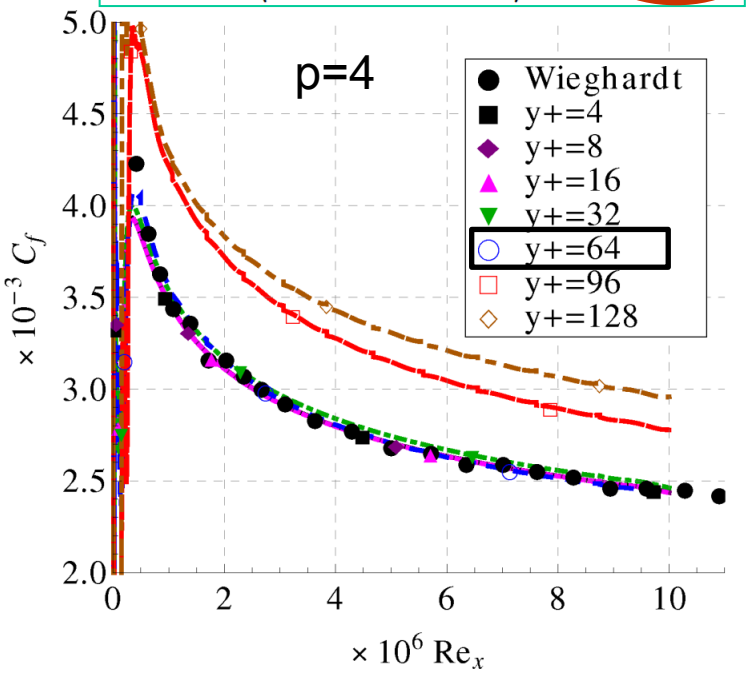

Convergence study – structured quads

- Friction coefficient Cf (numerical)
  - p=1 → $y^+ \approx 8$
  - p=2 → $y^+ \approx 16$
  - p=4 → $y^+ \approx 64$

p=1

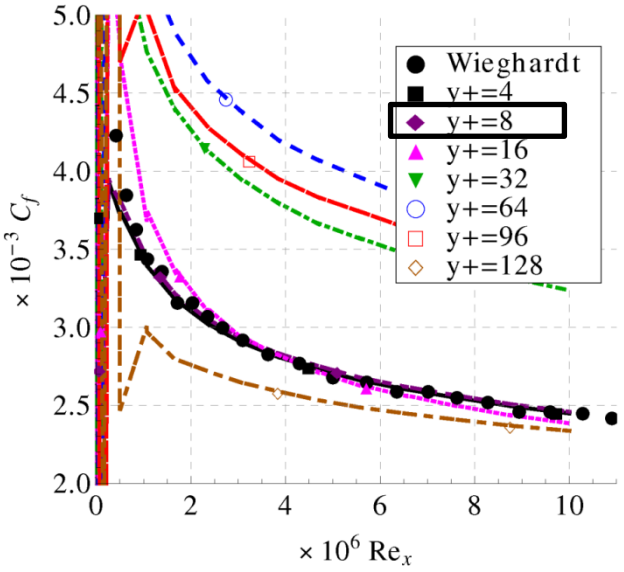

p=2

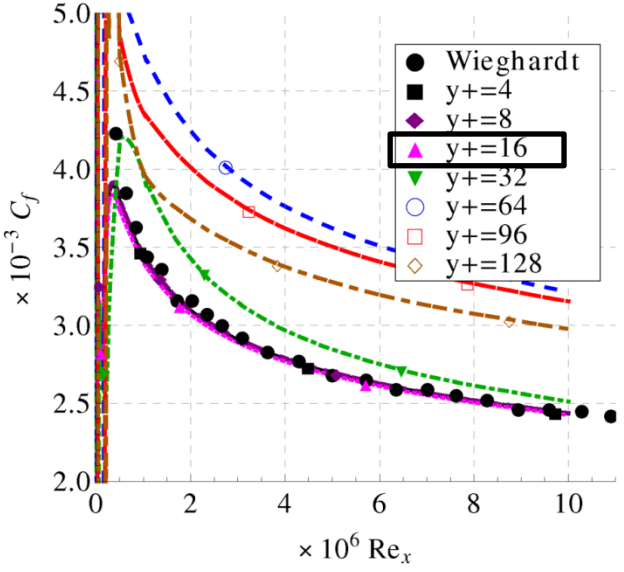

p=4

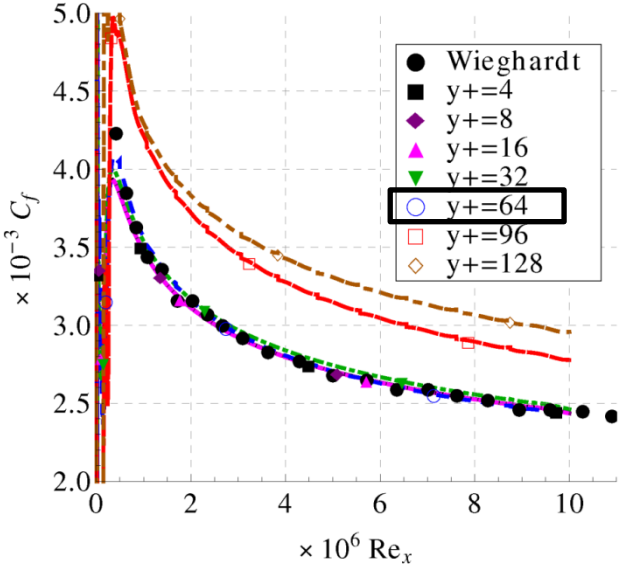

Convergence study – structured quads

- Velocity profiles $u^+(y^+)$
  - Boundary conditions (BC) are imposed weakly
  - Similar mesh resolutions as those based on the numerical friction
  - A very strict compliance with the no-slip BC is not required

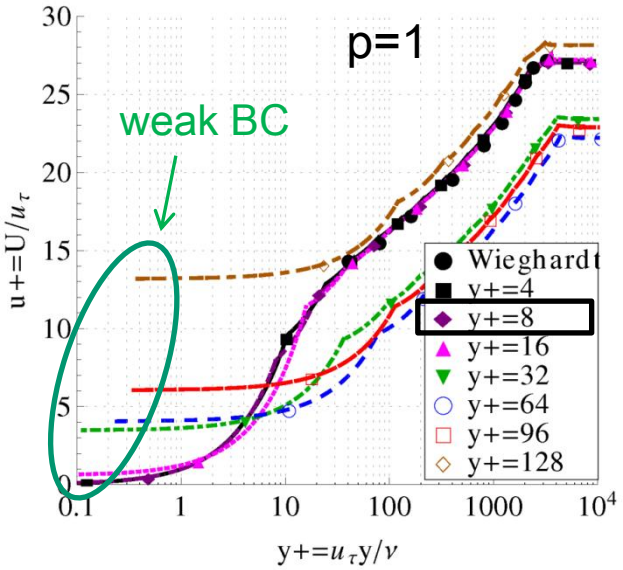

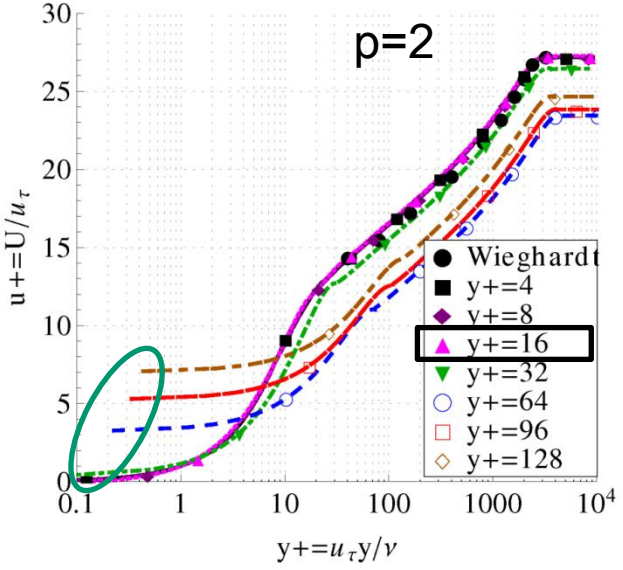

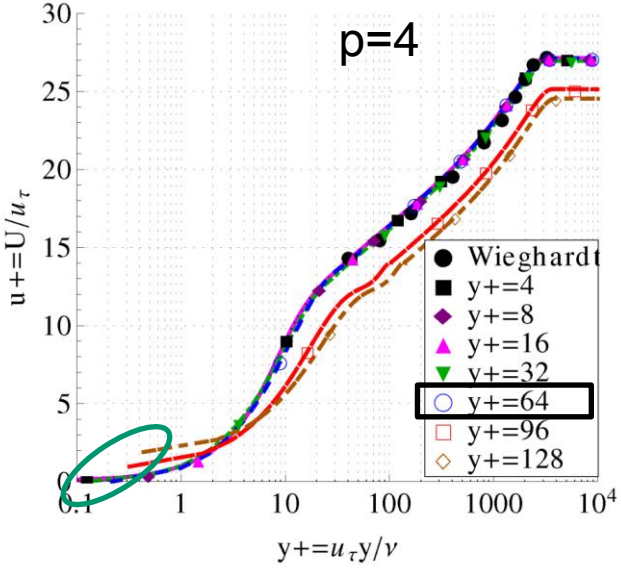

Convergence study – structured quads

- Turbulent viscosity profiles: $\bar{\mu} = \tilde{\mu}/(100\mu)$
  - **Close to the wall:** - no difference between P^1, P^2 and P^4-elements
  - **In the log-layer:** - larger spread of → *artificial thickening*
    - important undershoot → *stability*

p=1

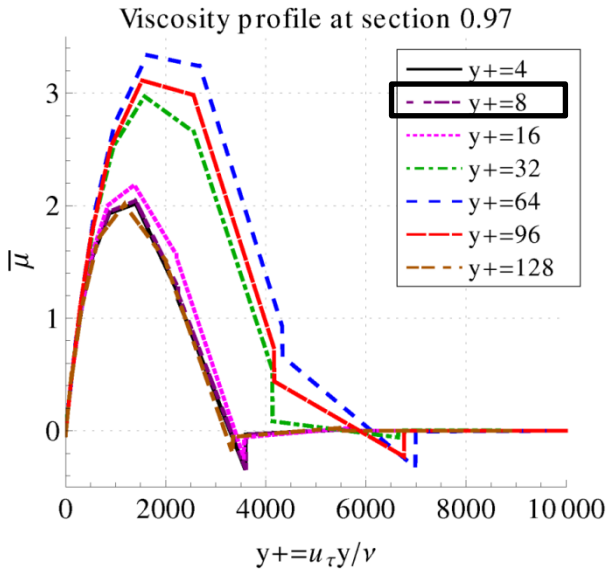

p=2

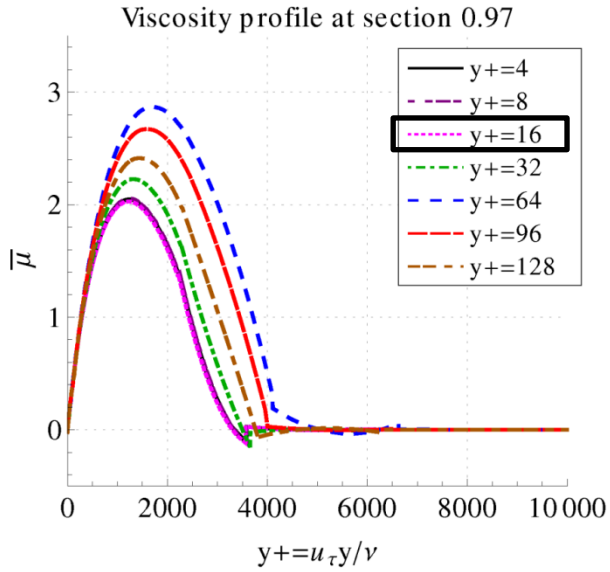

p=4

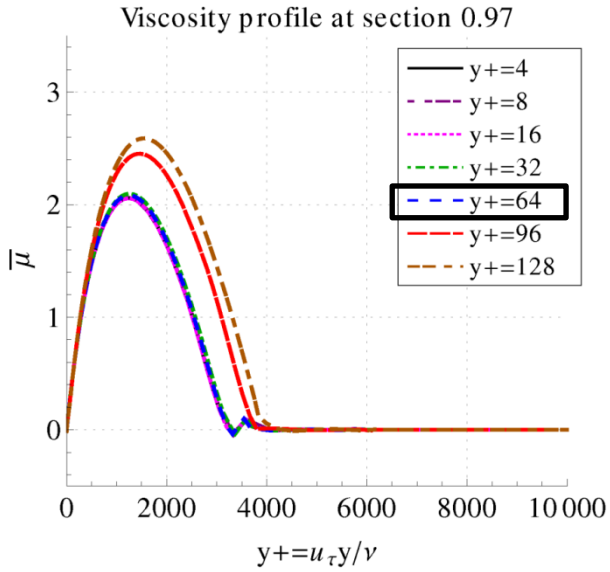

Comparison – quads vs triangles

- Skin friction
  - Smoother skin friction with quads
  - Reasons:
    1. Cf is proportional to ∂u/∂y
       ⇒ one order higher for quads
    2. No jump penalization between adjacent triangles that share only one node

Quads

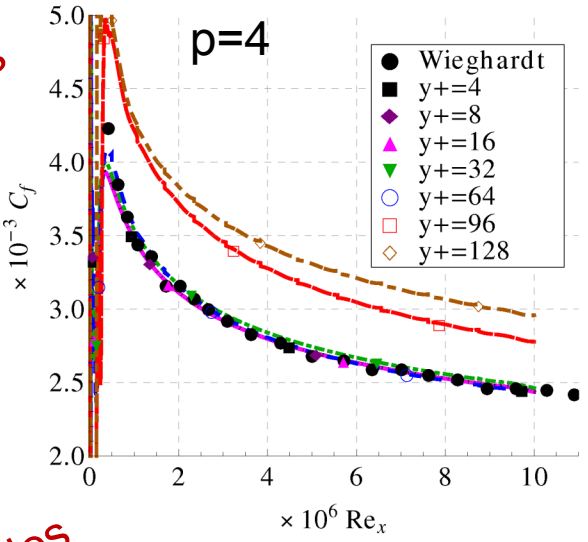

Triangles

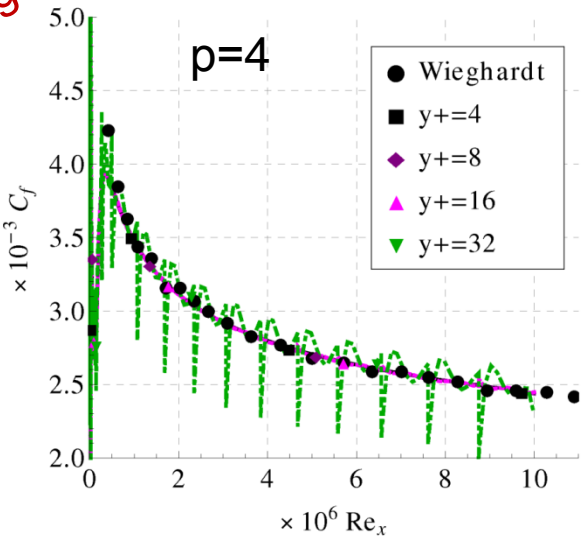

- Velocity profiles
  - No significant difference between quads and triangles
  - The no-slip condition is slightly better respected with triangles

High-order turbulent viscosity???

- Necessity of high-order polynomials to discretize the turbulence model?

1. Turbulent viscosity profiles (x=0.97)

p=3 (y^+=32)

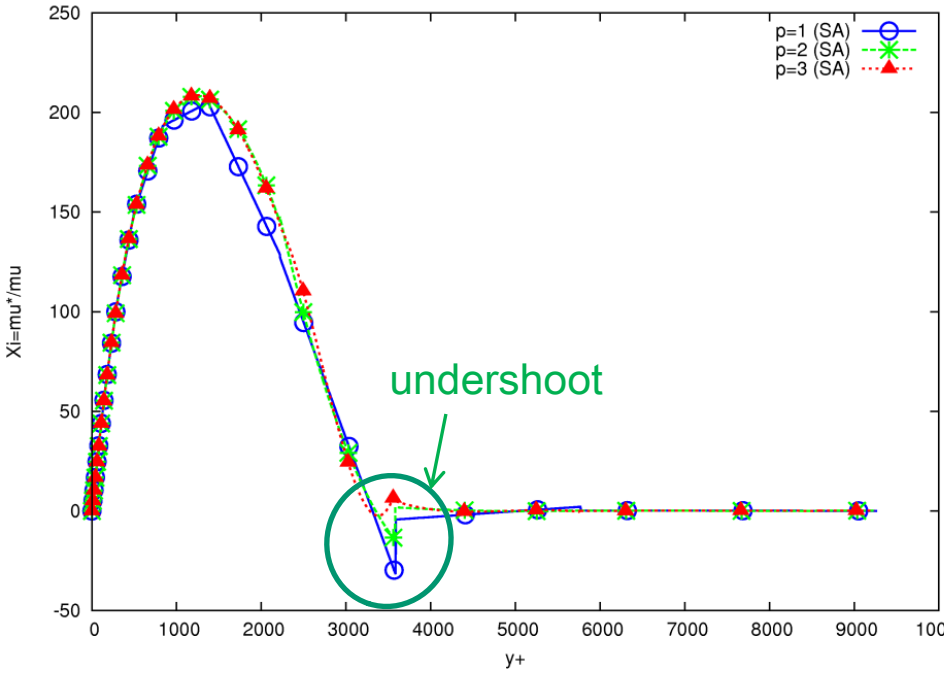

p=4 (y^+=64)

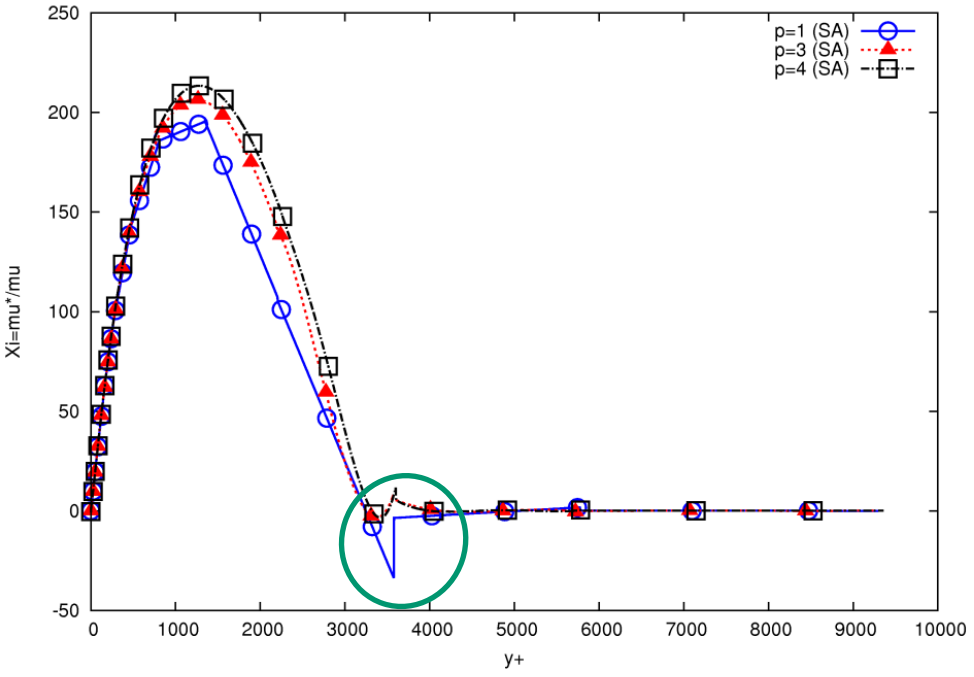

High-order turbulent viscosity???

2. Skin friction

p=3 (y^+=32)

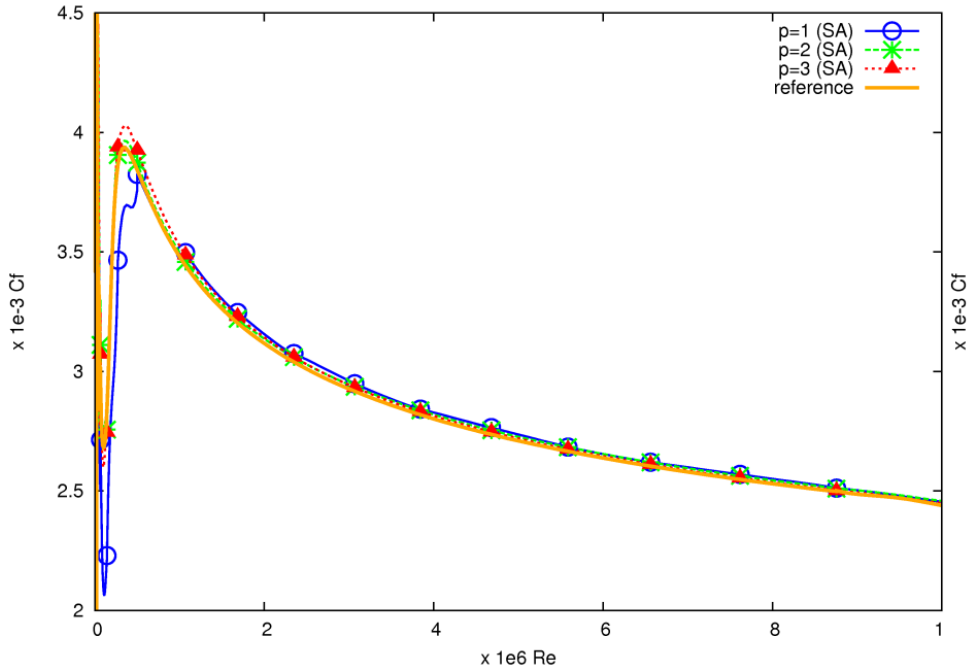

p=4 (y^+=64)

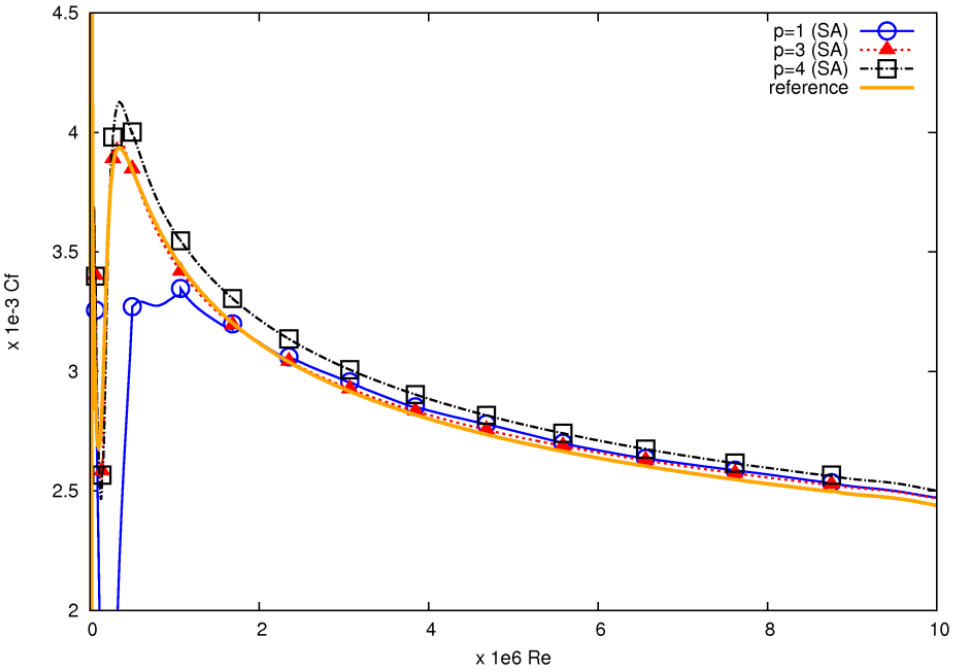

⇒ No significant impact

Effect of grid curvature – NACA 0012

- NACA 0012 (**α=3.59°**)
  - Re=1.86 $\times 10^6$, M_∞=0.3
  - 4th order geometry
  - 19 elements along the chord (2500 to 4800 elements)
- Observations
  - Good results for similar grid resolutions as in the case of straight elements, i.e. $y^+ \approx 50$ to 60 (p=4)
  - Accuracy of low-order polynomials decreases with increasing curvature

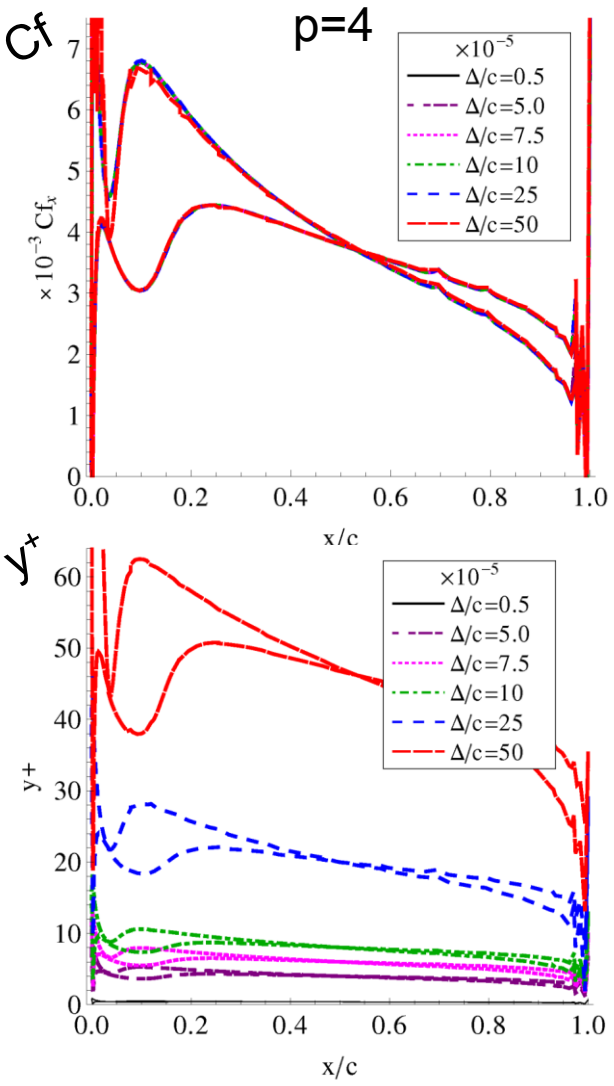

Test case: 3D high-lift cascade flow

- Description

  $Re = 8.4 \times 10^5$
  $M_\infty \approx 0,6$

- Grid specifications
  - Grid A
    - 42 000 hex
    - 52 800 prisms
    - 22 layers
  - Grid B
    - 17 800 hex
    - 19 400 prisms
    - 15 layers

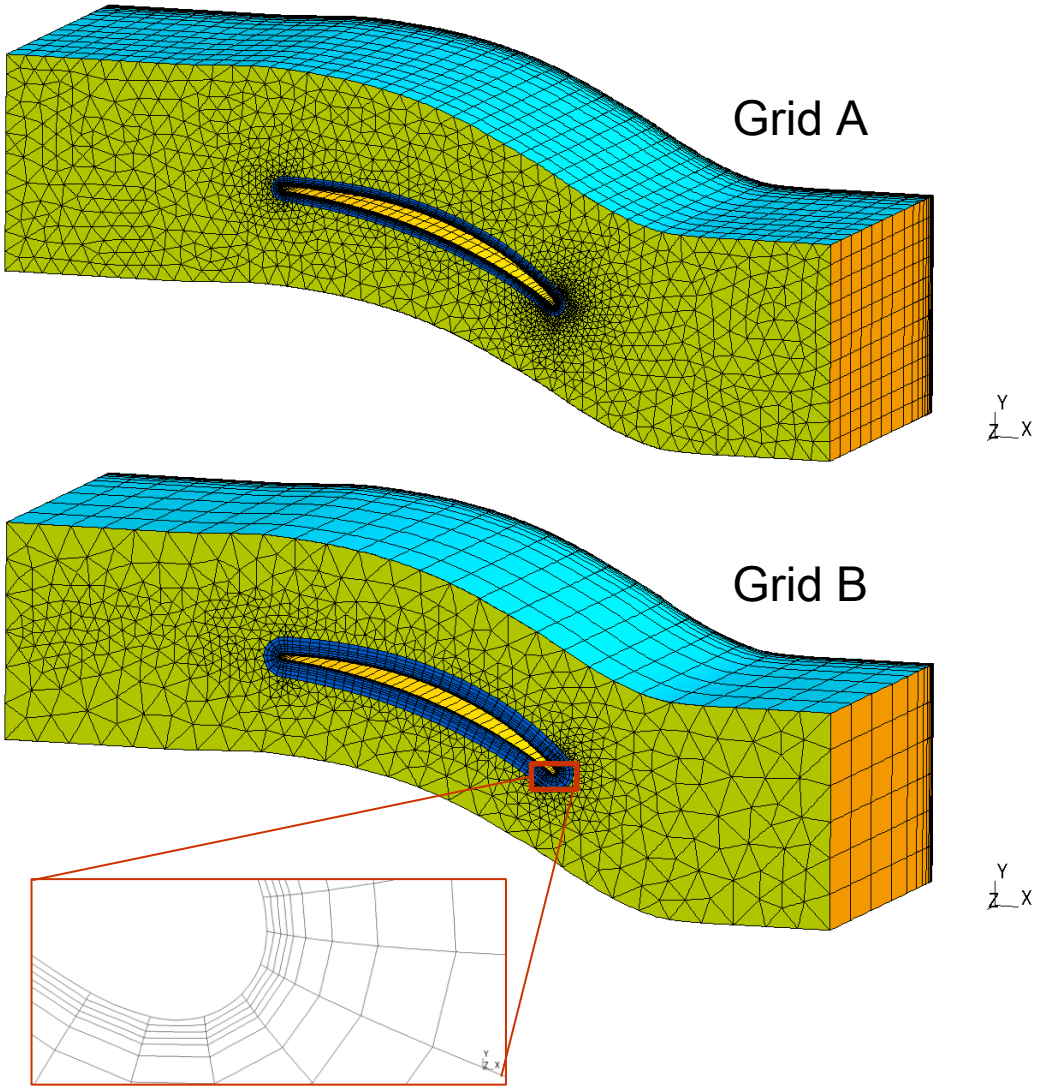

Test case: 3D high-lift cascade flow

- Mach number (p=2, gridA)

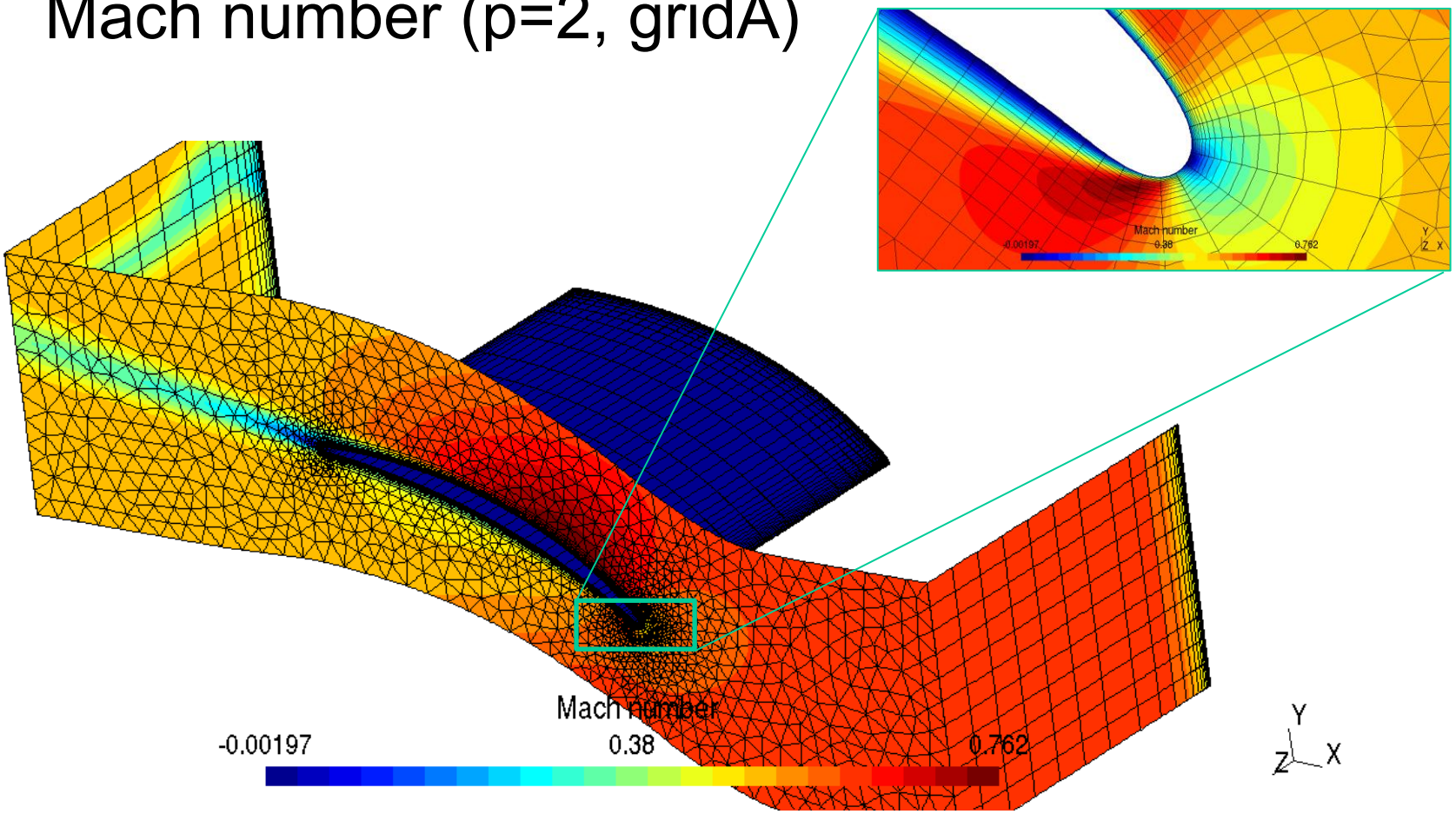

Test case: 3D high-lift cascade flow

Pressure

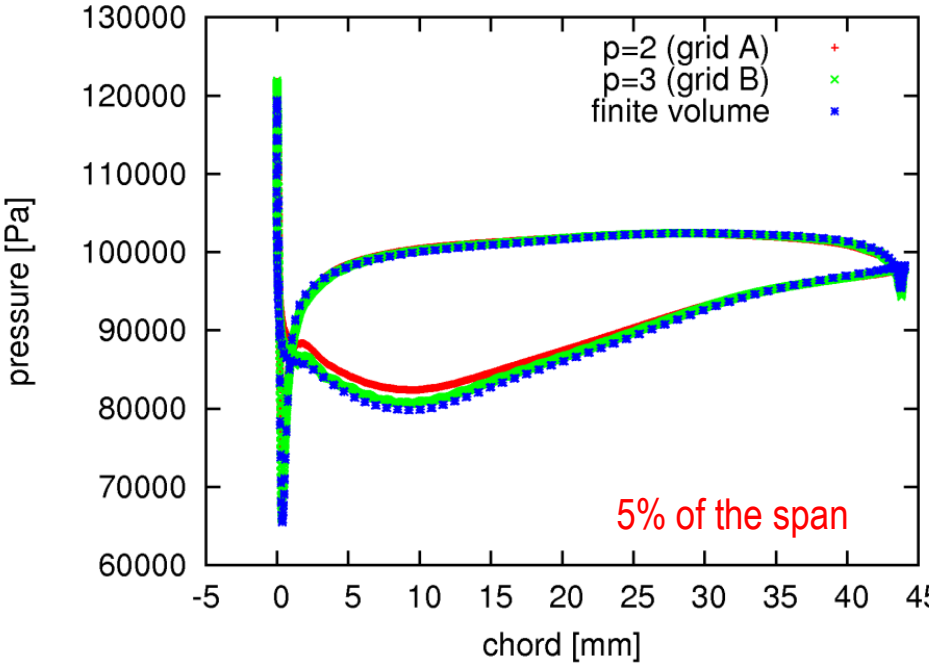

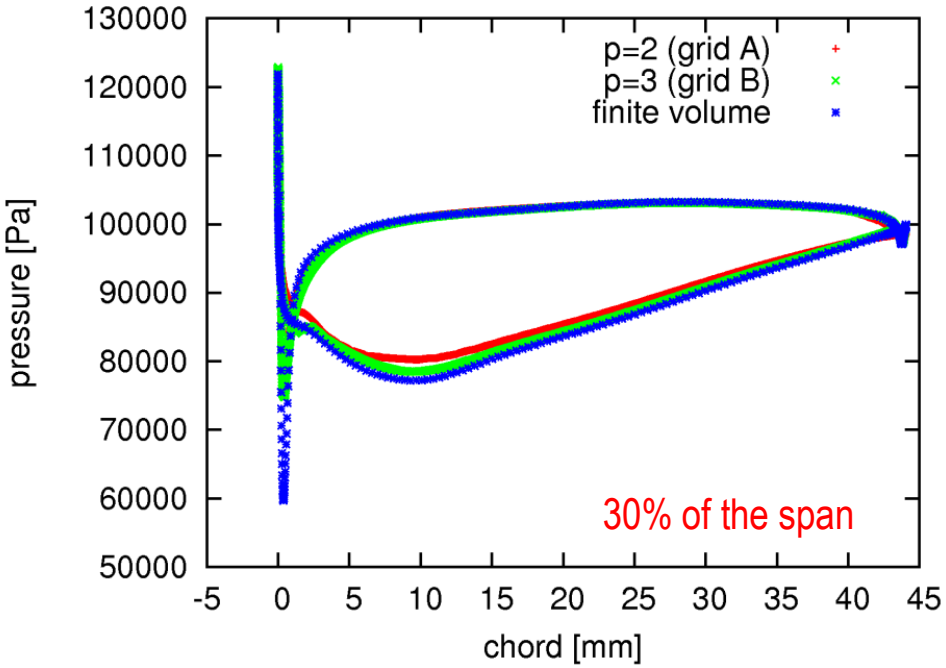

Conclusions

- Presented results
  - Adaptation of the SIPDG method to RANS computations
  - Grid resolution for turbulent boundary layers
  - Impact of lower order approximation of the turbulent viscosity
  - 3D high-lift cascade flows
- Future work
  - Improvement of the linear solver
  - Reduction of the memory consumption in 3D
  - Grid adaptation